Journal of Computational Design and Engineering 5 (2018) 232–242

Contents lists available at ScienceDirect

Journal of Computational Design and Engineering

journal homepage: www.elsevier.com/locate/jcde

# Thermal stratification effects on MHD radiative flow of nanofluid over nonlinear stretching sheet with variable thickness

Yahaya Shagaiya Daniel [a,b], Zainal Abdul Aziz [a,b,*], Zuhaila Ismail [a,b], Faisal Salah [c]

[a] Department of Mathematical Science, Faculty of Sciences, Universiti Teknologi Malaysia, 81310 UTM Johor Bahru, Johor, Malaysia
[b] UTM Centre for Industrial and Applied Mathematics, Institute Ibnu Sina for Scientific and Industrial Research, 81310 UTM Johor Bahru, Johor, Malaysia
[c] Department of Mathematics, Faculty of Science, University of Kordofan, Elobied 51111, Sudan

ARTICLE INFO

*Article history:*
Received 3 July 2017
Received in revised form 8 September 2017
Accepted 8 September 2017
Available online 19 September 2017

*Keywords:*
MHD nanofluid
Variable thickness
Thermal radiation
Similarity solution
Thermal stratification

ABSTRACT

The combined effects of thermal stratification, applied electric and magnetic fields, thermal radiation, viscous dissipation and Joules heating are numerically studied on a boundary layer flow of electrical conducting nanofluid over a nonlinearly stretching sheet with variable thickness. The governing equations which are partial differential equations are converted to a couple of ordinary differential equations with suitable similarity transformation techniques and are solved using implicit finite difference scheme. The electrical conducting nanofluid particle fraction on the boundary is passively rather than actively controlled. The effects of the emerging parameters on the electrical conducting nanofluid velocity, temperature, and nanoparticles concentration volume fraction with skin friction, heat transfer characteristics are examined with the aids of graphs and tabular form. It is observed that the variable thickness enhances the fluid velocity, temperature, and nanoparticle concentration volume fraction. The heat and mass transfer rate at the surface increases with thermal stratification resulting to a reduction in the fluid temperature. Electric field enhances the nanofluid velocity which resolved the sticking effects caused by a magnetic field which suppressed the profiles. Radiative heat transfer and viscous dissipation are sensitive to an increase in the fluid temperature and thicker thermal boundary layer thickness. Comparison with published results is examined and presented.



## 1. Introduction

More recently, a new class of fluids known as nanofluids has drawn attentions of researchers in diverse areas of science and engineering technology as result of wide coverage of industrial applications of these fluids. This new innovation aims at enhancing the thermal conductivities and the convective heat transfer of fluids through suspensions of ultrafine nanoparticles in the base fluids (Choi, 1995). Nanofluid is a mixture of an ultrafine nanoparticle of diameter less than 100 nm dispersed in the conventional basic fluid namely water, toluene, ethylene, and oil. Some common metallic nanoparticles are copper, silver, silicon, aluminum, and titanium which tends to enhances the thermal conductivities and hence convective heat transfer rate of such fluids, which increases the energy transport strength and enactment (Bhatti, Abbas, & Rashidi, 2017; Daniel, 2015; Hayat, Waqas, Shehzad, & Alsaedi, 2016; Kandasamy, Mohammad, Zailani, & Jaafar, 2017; Kumar, Sood, Sheikholeslami, & Shehzad, 2017; M'hamed et al., 2016). Considering variable thickness due to flow, it has gained consideration due to widely advances recently in the area of engineering enhancement in the fields of mechanical, civil, architectural, etc. (Hayat, Khan, Alsaedi, & Khan, 2017; Hayat, Shah, Alsaedi, & Khan, 2017; Khan, Hayat, Khan, & Alsaedi, 2017). This is rooted in the innovative work of Fang, Zhang, and Zhong (2012) against variable thickness using pure fluid. The surface medium of variable thickness have influential values and significant noticed in industrial and engineering processes. It aims at reducing the heaviness of supplementary component and enhance the operation of devices. Consequently, this drew the attention of various researchers (Hayat, Khan, Alsaedi, & Khan, 2016; Hayat et al., 2016; Khan, Hayat, Waqas, Khan, & Alsaedi, 2017; Khan, Khan, Waqas, Hayat, & Alsaedi, 2017; Khan, Waqas, Khan, Alsaedi, & Hayat, 2017; Waqas, Khan, Hayat, Alsaedi, & Khan, 2017) for flow behavior against stretching sheet involving variable thickness.

The study of nanofluids with effects of magnetic fields has enormous applications in the fields of metallurgy and engineering advancement (Alsaedi, Khan, Farooq, Gull, & Hayat, 2017; Daniel,

Peer review under responsibility of Society for Computational Design and Engineering.

* Corresponding author at: UTM Centre for Industrial and Applied Mathematics, Institute Ibnu Sina for Scientific and Industrial Research, 81310 UTM Johor Bahru, Johor, Malaysia.

*E-mail addresses:* shagaiya12@gmail.com (Y.S. Daniel), zainalaz@utm.my (Z.A. Aziz), zuhaila@utm.my (Z. Ismail), faisal19999@yahoo.com (F. Salah).

https://doi.org/10.1016/j.jcde.2017.09.001
2288-4300/

**Nomenclature**

| | |
|---|---|
| $b$ | positive constant [$s^{-1}$] |
| $B_0$ | uniform transverse magnetic field [N $m^{-1}$ $A^{-1}$] |
| $B$ | applied magnetic field |
| $c_f$ | skin friction coefficient |
| $c_p$ | specific heat constant [kJ/kg K] |
| $C_\infty$ | ambient concentration |
| $D_B$ | Brownian diffusion coefficient [$m^2$ $s^{-1}$] |
| $D_T$ | thermophoresis diffusion coefficient [$m^2$ $s^{-1}$] |
| $E_0$ | uniform electric field factor |
| $E_1$ | electrical field parameter |
| $E$ | applied electric field |
| $Ec$ | Eckert number |
| $f$ | dimensionless stream function |
| $h_f$ | heat transfer coefficient [W $m^{-2}$ $K^{-1}$] |
| $J$ | Joule current |
| $k, k_{nf}$ | thermal conductivity [W $m^{-1}$ $K^{-1}$] |
| $k_f, k_p$ | thermal conductivity of the base fluid and nanoparticle [W $m^{-1}$ $K^{-1}$] |
| $Le$ | Lewis number |
| $M$ | magnetic field parameter |
| $N$ | buoyancy ratio parameter |
| $Nb$ | Brownian motion parameter |
| $Nt$ | thermophoresis parameter |
| $Nu$ | local Nusselt number |
| $Pr$ | Prandtl number |
| $q_m$ | wall mass flux [kg $s^{-1}$ $m^{-2}$] |
| $q_r$ | radiative heat flux [W $m^{-2}$ ] |
| $q_w$ | wall heat flux [W $m^{-2}$ ] |
| $Rd$ | radiation parameter |
| $Re_x$ | local Reynolds number |
| $s_t$ | thermal stratification parameter |
| $Sh$ | local Sherwood number |
| $T$ | temperature of the fluid [K] |
| $T_0$ | reference temperature [K] |
| $T_W$ | constant temperature at the wall [K] |
| $T_\infty$ | ambient temperature [K] |
| $u, v$ | velocity component [m $s^{-1}$] |
| $x-$ and $y-$ | direction component [m] |
| $\bar{V}$ | velocity fluid [m $s^{-1}$] |
| $V_W$ | wall mass transfer [m $s^{-1}$] |

*Greek symbols*

| | |
|---|---|
| $\alpha$ | wall thickness parameter |
| $\alpha_f$ | the base fluid thermal diffusivity [$m^2$ $s^{-1}$] |
| $\sigma^*$ | Steffan-Boltzmann constant |
| $\sigma$ | electrical conductivity [S $m^{-1}$] |
| $\beta_{nf}$ | volumetric volume expansion coefficient of the nanofluid |
| $\eta$ | dimensionless similarity variable |
| $\mu$ | dynamic viscosity of the fluid [Pa s] |
| $\upsilon$ | kinematic viscosity of the fluid [$m^2$ $s^{-1}$] |
| $\rho, \rho_{nf}$ | density [kg $m^{-3}$] |
| $\rho_p$ | particle density [kg $m^{-3}$] |
| $(\rho)_f$ | density of the fluid [kg $m^{-3}$] |
| $(\rho c)_f$ | heat capacity of the fluid [J $kg^{-3}$ $K^{-1}$] |
| $(\rho c)_p$ | effective heat capacity of a nanoparticle [J $kg^{-3}$ $K^{-1}$] |
| $\psi$ | stream function |
| $\sigma$ | electrical conductivity |
| $\varphi$ | concentration of the fluid |
| $\varphi_W$ | nanoparticle volume fraction at the surface |
| $\varphi_\infty$ | nanoparticle volume fraction at large values of |
| $\theta$ | dimensionless temperature |
| $\phi$ | dimensionless concentration |
| $\tau$ | ratio between the effective heat transfer capacity and the heat capacity of the fluid |
| $\tau_W$ | surface shear stress |
| $\delta$ | chemical reaction parameter |

*Subscripts*

| | |
|---|---|
| $\infty$ | condition at the free stream |
| $W$ | condition at the wall/surface |

2015, 2016a, 2016b, 2017; Das, Sharma, & Sarkar, 2016; Hayat, Khan, Waqas, Alsaedi, & Yasmeen, 2017; Hayat, Khan, Waqas, Yasmeen, & Alsaedi, 2016; Hayat, Waqas, Khan, & Alsaedi, 2016, 2017; Khan et al., 2016; Raju, Reddy, Rao, & Rashidi, 2016; Waqas et al., 2016). Such significant are derived in stretching of plastic sheets, polymer industry and metallurgy by hydromagnetic. In the area of metallurgical processes which involves cooling of continuous strips/filaments through drawing them from nanofluid (Sheikholeslami & Shehzad, 2017a). Drawing these strips involves stretched at some point in time and also annealing and thinning of copper wires (Sheikholeslami & Shehzad, 2017b). In these process, the desired properties of final product strongly depend by the virtue on the level of cooling from side to side drawing such strips in an electrically conducting fluid with impacts of magnetic fields (Hayat, Qayyum, Shehzad, & Alsaedi, 2017). Nanofluids are primarily aimed at cooling devices in the computer (cooling of microchips) and electronics devices (microfluidic) applications. Investigation showed that nanofluids with the influence of magnetic field, by varying the electromagnetic field, it absorbs energy and gives a controllable hyperthermia, which acts as super-para-magnetic fluid see the works of Hussain, Shehzad, Hayat, and Alsaedi (2015).

In different flows of practical relevance in nature as well as in many engineering devices, the environment is thermally stratified (Daniel, Aziz, Ismail, & Salah, 2017a). Stratification is a formation or deposition of layers which occur as results of temperature difference or variations of densities or due to the presence of different fluids. The discharge of hot fluid into enclosed regions more often leads in a stable thermal stratification containing lighter fluid overlying denser fluid (Besthapu, Haq, Bandari, & Al-Mdallal, 2017). These thermal stratification influence of convective heat transfer due to stretching sheet is of paramount importance in polymer extrusion processes, the object after passing through a die, enters the fluid for cooling of at certain range of temperature (Alsaedi et al., 2017). The level at which these objects are cooled a vital bearing in mind on the desired properties of the finished product. These applications involve heat rejection into the environment namely lakes, seas, and rivers; thermal energy storage systems like solar ponds; and heat transfer through thermal sources namely condensers of power plants (Hayat, Nassem, Khan, Farooq, & Al-Saedi, 2017; Hayat, Rashid, Imtiaz, & Alsaedi, 2017; Malik, Bilal, Bibi, & Ali, 2017).

Related works pointed out that thermal stratification effects in electrical magnetohydrodynamic (MHD) boundary layer stretched flow of revised nanofluid model (Kuznetsov & Nield, 2013) containing nanoparticles with water base fluid due to variable thickness is not investigated yet. Consequently, our main goal here is four folds. Firstly to examine thermal stratification effects through the heat in the magnetohydrodynamic (MHD) flow. Secondly to analyze electric field impact. Thirdly to address thermal radiation and Joule heating in view of Heat transfer phenomenon. Fourth to present formulation in the company of Brownian motion and thermophoresis. In manufacturing processes, the raw material passes through the die for the extrusion in a liquefied state under high

temperature, with densities gradient leads to thermal stratification. Moving surface into a cooling medium is a mathematical tool for the process of heat treatment in the fields of engineering technology noticed in mechanical, civil, architectural involved variable thickness. The governing mathematical system which is partial differential equations is converted to a system of nonlinear coupled of ordinary differential equations by similarity transformation techniques. The resulted non-dimensional nonlinear convective effect are solved using implicit finite difference. Behaviors of various pertinent parameters on the velocity, temperature, and nanoparticle concentration are examined. Skin friction coefficient and Nusselt number are compared and analyzed. A comparative assessment of the present and previous data is made with judgment.

## 2. Mathematical formulation

### 2.1. Flow formulation

Consider a steady two-dimensional flow of magnetohydrodynamic (MHD) nanofluid due to a nonlinearly stretching sheet with variable thickness. The velocity of the stretching sheet is denoted as $U_W(x) = U_0(x+b)^n$, and the surface is taken at $y = A_1(x+b)^{\frac{1-n}{2}}$ as the nonlinear stretching surface variable, in which for $n = 1$ the stretching sheet is of the same thickness. The boundary layer equations of the fluid flow are consist of the continuity equation, the momentum equation, energy equation and concentration equation. The laminar incompressible flow of viscous nanofluid in the presence of applied magnetic field $B$ and electric field $E$ are taken into consideration. The flow is due to stretching of a sheet from a slot through two equal and opposite force and thermally radiative. The magnetic and electric fields obey the Ohm's law define $\bar{J} = \sigma(\bar{E} + \bar{V} \times \bar{B})$ where $\bar{J}$ is the Joule current, $\sigma$ is the electrical conductivity and represent the fluid velocity. The magnetic field of strength $B(x)$ and electric field of strength $E(x)$ is applied normal to the flow field. The induced magnetic field is so small, so the induced magnetic field and Hall current impacts are insignificant. We choose the Cartesian coordinate system such that $u$ and $v$ are the velocity components of the fluid in the $x$ and $y$-direction see Fig. 1. The combined effects of thermal radiation, viscous dissipation, magnetic and electrical fields are incorporated. The nanofluid flow due to a nonlinear stretching sheet with variable thickness is considered. The investigation of the nanofluid which involves particles and liquid. The fluid properties are indicated with subscript as $(\rho c_p)_f$ and that of particles properties as $(\rho c_p)_p$. The magnetohydrodynamic (MHD) boundary layer flow equation of an incompressible nanofluid are given as:

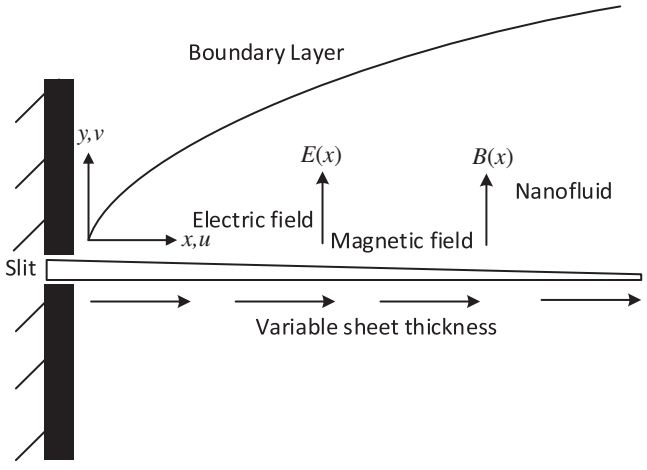


**Fig. 1.** Physical configuration of the geometry.

$$\frac{\partial u}{\partial x} + \frac{\partial v}{\partial y} = 0 \tag{1}$$

$x$-direction momentum equation

$$u\frac{\partial u}{\partial x} + v\frac{\partial u}{\partial y} = -\frac{1}{\rho_f}\frac{\partial P}{\partial x} + \nu\left(\frac{\partial^2 u}{\partial x^2} + \frac{\partial^2 u}{\partial y^2}\right) + \frac{\sigma}{\rho_f}(E(x)B(x) - B^2(x)u) \tag{2}$$

$y$-direction momentum equation

$$u\frac{\partial v}{\partial x} + v\frac{\partial v}{\partial y} = -\frac{1}{\rho_f}\frac{\partial P}{\partial y} + \nu\left(\frac{\partial^2 v}{\partial x^2} + \frac{\partial^2 v}{\partial y^2}\right) + \frac{\sigma}{\rho_f}(E(x)B(x) - B^2(x)v) \tag{3}$$

The uniqueness for this, the electrical conducting nanofluid in the presence of applied magnetic and electric fields which are incorporated in the governing equation of the nanofluid flow field. The electrically conducting implies the nanofluid possess electricity force and it may make the fluid heat transfer impact changeable, fluid due to nonlinear stretching sheet with variable thickness with defined variables for magnetic field factor $B(x) = B_0(x+b)^{(n-1)/2}$, $\sigma$ is the electrical conductivity, $E(x) = E_0(x+b)^{(n-1)/2}$ is the electrical field factor, $\nu, \rho_f$ are the kinematic viscosity of the fluid and the fluid density. Follow with the boundary conditions for the velocity component (Hayat, Khan, Farooq, Yasmeen, & Alsaedi, 2016):

$$\begin{aligned} &y = A_1(x+b)^{\frac{(1-n)}{2}}, u = U_W(x) = U_0(x+b)^n, v = 0 \\ &y \to \infty : u \to 0 \end{aligned} \tag{4}$$

where $b$ is the stretching sheet constant, $n$ is the power law index, and $W$ is the wall notation. To obtain similarity solution of equations (1)–(3) the nondimensionalized variables are presented as (Hayat, Khan, Waqas, & Alsaedi, 2017; Khan, Hayat, Waqas, & Alsaedi, 2017; Khan, Waqas, Hayat, & Alsaedi, 2017):

$$\begin{aligned} &\psi = \left(\frac{2}{n+1}\nu U_0(x+b)^n\right)^{1/2} F(\xi), \xi = y\left(\frac{n+1}{2\nu}U_0(x+b)^{n-1}\right)^{1/2}, \\ &\phi(\eta) = (\varphi - \varphi_\infty)/\varphi_\infty \\ &v = -\left(\frac{n+1}{2}\nu U_0(x+b)^{n-1}\right)^{1/2}\left(F(\xi) + \xi\frac{n-1}{n+1}F'^{(\xi)}\right), \\ &\theta(\eta) = (T - T_\infty)/(T_W - T_\infty), \\ &u = U_0(x+b)^n F(\xi), \end{aligned} \tag{5}$$

Using an order magnitude analysis of the $y$-direction momentum equation (normal to the stretching sheet) applying the normal boundary layer equation:

$$\begin{aligned} &u \gg v \\ &\frac{\partial u}{\partial y} \gg \frac{\partial u}{\partial x}, \frac{\partial v}{\partial x}, \frac{\partial v}{\partial y} \\ &\frac{\partial p}{\partial y} = 0. \end{aligned} \tag{6}$$

After the boundary layer equation (Daniel, Aziz, Ismail, & Salah, 2017c, 2017d, 2017e; Daniel et al., 2017a), substitute equations (5) and (6) into (1)–(3), we obtained the transformed ordinary differential equation as:

$$F'''(\xi) + F(\xi)F''(\xi) - \frac{2n}{n+1}(F'(\xi))^2 + M(E_1 - F'(\xi)) = 0 \tag{7}$$

Here $F(\xi)$ is the dimensionless velocity, $M = 2\sigma B_0^2/\rho_f U_0(n+1)$ is the magnetic field parameter, $E_1 = E_0/B_0U_0(x+b)^n$ is the electric parameter. The transformed boundary conditions are presented as:

$$\xi = 0: \quad F(\xi) = \alpha\frac{1-n}{1+n}, \quad F'(\xi) = 1,$$
$$\xi \to \infty: \quad F'(\xi) = 0 \tag{8}$$

Here $\alpha = A_1\left(\frac{n+1}{2}\frac{U_0}{\nu}\right)^{1/2}$. Taking $F(\xi) = f(\xi - \alpha) = f(\eta)$. The above Eqs. (7) and (8) becomes:

$$f'''(\eta) + f(\eta)f''(\eta) - \frac{2n}{n+1}(f'(\eta))^2 + M(E_1 - f'(\eta)) = 0 \tag{9}$$

Boundary conditions

$$f(0) = \alpha\frac{1-n}{1+n}, \quad f'(0) = 1, \quad f'(\infty) = 0 \tag{10}$$

where $\alpha$ is the wall thickness parameter. The skin friction coefficient is defined in terms of shear stress and density:

$$c_f = \frac{\tau_w}{\rho U_w^2(x)} \tag{11}$$

where $\tau_w$ is the surface shear stress expressed in terms of $\mu$ dynamic viscosity of the fluid stretching surface defined as

$$\tau_w = \mu\left(\frac{\partial u}{\partial y}\right)\Big|_{y=A_1(x+b)^{\frac{(1-n)}{2}}} \tag{12}$$

For the local skin-friction coefficient is presented in non-dimensional form as

$$Re_x^{1/2}c_{fx} = \sqrt{\frac{1+n}{2}}f''(0) \tag{13}$$

Here $Re_x = A_1(x+b)^{n+1}/\nu = U_W(x+b)/\nu$ is the local Reynolds number.

### 2.2. Heat convection formulation

The energy field for temperature can be expressed in terms of thermal radiation, thermal stratification, viscous dissipation and the Joule heating as (Farooq et al., 2016; Hayat, Khan, Farooq, Alsaedi, & Yasmeen, 2017; Hayat, Khan, Imtiaz, Alsaedi, & Waqas, 2016; Hayat, Khan, Waqas, Alsaedi, & Farooq, 2017):

$$u\frac{\partial T}{\partial x} + v\frac{\partial T}{\partial y} = \frac{k}{\rho c_p}\left(\frac{\partial^2 T}{\partial x^2} + \frac{\partial^2 T}{\partial y^2}\right) + \tau\left\{D_B\left(\frac{\partial \varphi}{\partial x}\frac{\partial T}{\partial x} + \frac{\partial \varphi}{\partial y}\frac{\partial T}{\partial y}\right) + \frac{D_T}{T_\infty}\left[\left(\frac{\partial T}{\partial x}\right)^2 + \left(\frac{\partial T}{\partial y}\right)^2\right]\right\} - \frac{1}{(\rho c)_f}\left(\frac{\partial q_r}{\partial y}\right) + \frac{\mu}{\rho c_p}\left(\frac{\partial u}{\partial y}\right)^2 + \frac{\sigma}{\rho c_p}(uB(x) - E(x))^2 \tag{14}$$

where $T, \varphi$ is the fluid temperature and concentration, the ambient values of temperature and nanoparticle fraction attained to a constant value of $T_\infty$ and $\varphi_\infty$. The radiative heat flux $q_r$ via Rosseland approximation can be written as (Daniel, Aziz, Ismail, & Salah, 2017b; Daniel & Daniel, 2015);

$$q_r = -\frac{4\sigma^*}{3k^*}\frac{\partial T^4}{\partial y} \tag{15}$$

We assumed less temperature gradient within the viscous fluid flow in such a way that $T^4$ can be expressed as a linear function of temperature. By expanding $T^4$ using Taylor's series approach about a free stream temperature $T_\infty$. Neglecting higher order terms in the above equation which resulted to an approximated:

$$T^4 \cong 4T_\infty^3 T - 3T_\infty^4. \tag{16}$$

Using Eqs. (15) and (16) into Eq. (14), we have,

$$u\frac{\partial T}{\partial x} + v\frac{\partial T}{\partial y} = \frac{k}{\rho c_p}\left(\frac{\partial^2 T}{\partial x^2} + \frac{\partial^2 T}{\partial y^2}\right) + \tau\left\{D_B\left(\frac{\partial \varphi}{\partial x}\frac{\partial T}{\partial x} + \frac{\partial \varphi}{\partial y}\frac{\partial T}{\partial y}\right) + \frac{D_T}{T_\infty}\left[\left(\frac{\partial T}{\partial x}\right)^2 + \left(\frac{\partial T}{\partial y}\right)^2\right]\right\} + \frac{16\sigma^* T_\infty^3}{3k^*\rho c_p}\frac{\partial^2 T}{\partial y^2} + \frac{\mu}{\rho c_p}\left(\frac{\partial u}{\partial y}\right)^2 + \frac{\sigma}{\rho c_p}(uB(x) - E(x))^2 \tag{17}$$

**Table 1**
Comparison of $-f''(0)$ when $\alpha = 0.25, \& E_1 = M = 0$ for varying values of $m$.

| $n$ | Fang et al. (2012) $-f''(0)$ | Present result |
|---|---|---|
| 10.00 | 1.1433 | 1.143332 |
| 9.00 | 1.1404 | 1.140404 |
| 7.00 | 1.1323 | 1.132297 |
| 5.00 | 1.1186 | 1.118601 |
| 3.00 | 1.0905 | 1.090503 |
| 1.00 | 1.0000 | 1.000008 |
| 0.50 | 0.9338 | 0.933832 |
| 0.00 | 0.7843 | 0.784284 |
| −1/3 | 0.5000 | 0.500001 |
| −0.5 | 0.0833 | 0.083322 |
| −0.51 | 0.0385 | 0.038525 |
| −0.55 | −0.1976 | −0.197610 |
| −0.60 | −0.8503 | −0.850207 |
| −0.61 | −1.2244 | −1.224426 |

**Table 2**
Comparison of $-f''(0)$ when $\alpha = 0.5, \& E_1 = M = 0$ for varying values of $m$.

| $n$ | Fang et al. (2012) $-f''(0)$ | Present result |
|---|---|---|
| 10.00 | 1.0603 | 1.060342 |
| 9.00 | 1.0589 | 1.058933 |
| 7.00 | 1.0550 | 1.055061 |
| 5.00 | 1.0486 | 1.048627 |
| 3.00 | 1.0359 | 1.035883 |
| 2.00 | 1.0234 | 1.023420 |
| 1.00 | 1.0000 | 1.000008 |
| 0.50 | 0.9799 | 0.979950 |
| 0.00 | 0.9576 | 0.957646 |
| −1/3 | 1.0000 | 1.000000 |
| −0.5 | 1.1667 | 1.166661 |
| −0.51 | 1.1859 | 1.185899 |
| −0.55 | 1.2807 | 1.280724 |
| −0.60 | 1.4522 | 1.452177 |
| −0.70 | 2.0967 | 2.096621 |

**Table 3**
Numerical values for Skin friction for different values of $M, E_1, n, \& \alpha$ when.

| $M$ | $n$ | $E_1$ | $\alpha$ | $-f''(0)$ |
|---|---|---|---|---|
| 0.1 | 2.0 | 0.1 | 0.25 | 1.079498 |
| 0.5 | | | | 1.177340 |
| 1.0 | | | | 1.299003 |
| 1.5 | | | | 1.412475 |
| 0.1 | 3.0 | | | 1.109261 |
| | 5.0 | | | 1.137842 |
| | 7.0 | | | 1.151717 |
| | 2.0 | 0.2 | | 1.055921 |
| | | 0.3 | | 1.033923 |
| | | 0.4 | | 1.012958 |
| | | 0.1. | 0.5 | 1.043214 |
| | | | 0.75 | 1.008310 |
| | | | 1.0 | 0.974764 |
| | | | 1.25 | 0.942551 |

Here $\alpha_f = k/\rho c_p, \mu, \sigma^*, \rho\rho_f$, and $\rho_p$ is the fluid thermal diffusivity, the kinematic viscosity, the Steffan-Boltzmann constant, the density, the fluid density and particles density respectively. We also have $B_0, D_B, D_T, \tau = (\rho c)_p/(\rho c)_f$ which represents the magnetic field factor, the Brownian diffusion coefficient, the thermophoresis diffusion coefficient, the ratio between the effective heat transfer capacity of the ultrafine nanoparticle material and the heat capacity of the fluid. The boundary conditions are defined as:

**Table 4**
Numerical values for local Nusselt number for different values of $M, Rd, Ec, Le, Nb, Nt, Pr, n, E_1, \& s_t$ when $\alpha = 0.25$.

| $M$ | $Rd$ | $Ec$ | $Le$ | $Nb$ | $Nt$ | $n$ | $E_1$ | $s_t$ | $Pr$ | $-\theta'(0)$ |
|---|---|---|---|---|---|---|---|---|---|---|
| 0.1 | 0.2 | 0.1 | 1.5 | 0.1 | 0.1 | 2.0 | 0.1 | 0.1 | 0.72 | 0.721557 |
| 0.5 | | | | | | | | | | 0.725550 |
| 1.0 | | | | | | | | | | 0.715291 |
| 1.5 | | | | | | | | | | 0.704856 |
| 0.1 | 0.4 | | | | | | | | | 0.638225 |
| | 0.6 | | | | | | | | | 0.574814 |
| | 0.8 | | | | | | | | | 0.524756 |
| | 1.0 | | | | | | | | | 0.484152 |
| | 0.2 | 0.2 | | | | | | | | 0.700506 |
| | | 0.4 | | | | | | | | 0.658399 |
| | | 0.6 | | | | | | | | 0.616286 |
| | | 0.8 | | | | | | | | 0.574166 |
| | | 0.1 | 1.7 | | | | | | | 0.721933 |
| | | | 2.0 | | | | | | | 0.722432 |
| | | | 2.5 | | | | | | | 0.723135 |
| | | | 3.0 | | | | | | | 0.723719 |
| | | | 10 | 0.2 | | | | | | 0.727572 |
| | | | | 0.3 | | | | | | 0.727572 |
| | | | | 0.4 | | | | | | 0.727572 |
| | | | | 0.1 | 0.2 | | | | | 0.739844 |
| | | | | | 0.3 | | | | | 0.752317 |
| | | | | | 0.4 | | | | | 0.764990 |
| | | | | | 0.1 | 3.0 | | | | 0.753037 |
| | | | | | | 4.0 | | | | 0.767716 |
| | | | | | | 5.0 | | | | 0.777263 |
| | | | | | | 2.0 | 0.2 | | | 0.748429 |
| | | | | | | | 0.3 | | | 0.763959 |
| | | | | | | | 0.4 | | | 0.776391 |
| | | | | | | | 0.1 | 0.2 | | 0.707060 |
| | | | | | | | | 0.3 | | 0.686655 |
| | | | | | | | | 0.4 | | 0.666356 |
| | | | | | | | | 0.1 | 1.0 | 0.895679 |
| | | | | | | | | | 3.0 | 1.706871 |
| | | | | | | | | | 5.0 | 2.248331 |
| | | | | | | | | | 7.0 | 2.674167 |

When $y = A_1(x+b)^{\frac{(1-n)}{2}} : T = T_W = T_0 + c(x+b)^n$,

$$y \to \infty : T \to T_\infty = T_0 + d(x+b)^n, \tag{18}$$

Here $T_0$ is the reference temperature, $c > 0 \& d > 0$ are constants. The transformed energy equation after applying boundary layer approximation is presented as:

$$\left(1+\frac{4}{3}Rd\right)\theta'' + Pr\left(f\theta' - \frac{2n}{n+1}f'\theta + Nb\phi'\theta' + Nt\theta'^2 + Ec(f'')^2 + MEc(f'-E_1)^2 - \frac{2n}{n+1}s_t f'\right) = 0 \tag{19}$$

Boundary conditions

$$\theta(0) = 1 - s_t, \theta(\infty) = 0 \tag{20}$$

Here $Pr = \mu c_p/k$ is the Prandtl number, $Nb = (\rho c)_p D_B \varphi_\infty/(\rho c)_f \nu$ is the Brownian motion parameter,$Nt = (\rho c)_p D_T(T_w - T_\infty)/(\rho c)_f \nu T_\infty$ is the thermophoresis parameter, $Ec = U_W^2/c_p(T_w - T_\infty)$ is the Eckert number, $s_t = c/d$ is the thermal stratification parameter, and $Rd = 4\sigma^* T_\infty^3/k^* k$ is the radiation parameter. These parameters affect the flow behavior, the rate of heat and mass transfer. The physical importance of Brownian motion which is about the diffusion equation produces an approximation of the time generation of the density function corresponding to the position of the particles moving under the Brownian motion.

Nusselt number is defined as:

$$Nu_x = (x+b)^{\frac{(1-n)}{2}} q_w/k(T_W - T) \tag{21}$$

where $q_w$ is the wall heat flux given as:

$$q_W = -(k + \frac{16\sigma^* T_\infty^3}{3k^*})\frac{\partial T}{\partial y}\Big|_{y=A_1(x+b)^{\frac{(1-n)}{2}}} \tag{22}$$

By using above equations we get the dimensionless form as:

$$Nu_x(Re_x)^{-1/2} = -\left(1+\frac{4}{3}Rd\right)\sqrt{\frac{1+n}{2}}\theta'(0) \tag{23}$$

### 2.3. Volume fraction concentration formulation

The mass diffusion analysis for the boundary layer flow of the nanoparticle fraction $\varphi$ with energy field for temperature $T$ is presented as:

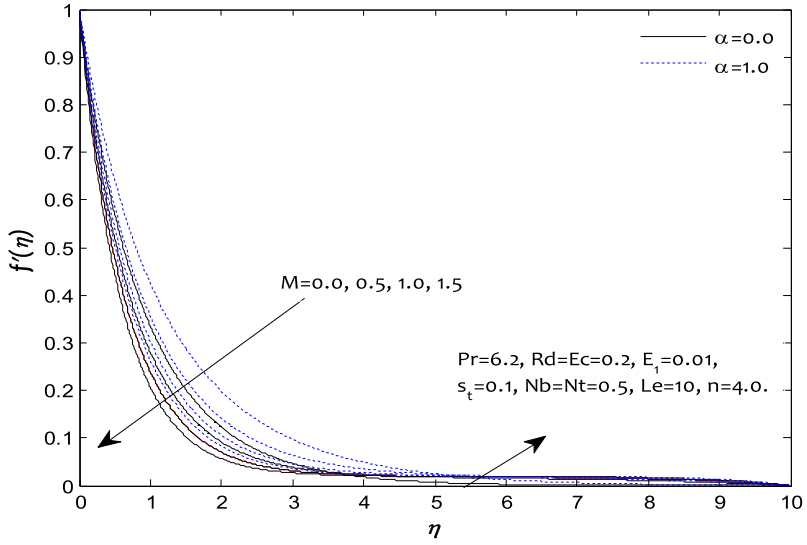


**Fig. 2.** Influence of $M$ on the velocity profile $f'(\eta)$.

$$u\frac{\partial\varphi}{\partial y}+v\frac{\partial\varphi}{\partial y}=D_B\left(\frac{\partial^2\varphi}{\partial x^2}+\frac{\partial^2\varphi}{\partial y^2}\right)+\frac{D_T}{T_\infty}\left(\frac{\partial^2 T}{\partial x^2}+\frac{\partial^2 T}{\partial y^2}\right) \tag{24}$$

After applying the boundary layer approximation to equation (27), it reduces to:

$$u\frac{\partial\varphi}{\partial y}+v\frac{\partial\varphi}{\partial y}=D_B\left(\frac{\partial^2\varphi}{\partial y^2}\right)+\frac{D_T}{T_\infty}\left(\frac{\partial^2 T}{\partial y^2}\right) \tag{25}$$

Subjected to boundary conditions:

When $y=A_1(x+b)^{\frac{(1-n)}{2}}: D_B\frac{\partial\varphi}{\partial y}+\frac{D_T}{T_\infty}\frac{\partial T}{\partial y}=0$

$$y\to\infty:\varphi\to\varphi_\infty \tag{26}$$

Applying the similarity variables defined in Eq. (6) into Eq. (28) the dimensionless concentration resulted as:

$$\phi''+\frac{Nt}{Nb}\theta''+Lef\phi'=0 \tag{27}$$

Boundary conditions:

$$Nb\phi'(0)+Nt\theta'(0)=0,\ \ \phi(\infty)=0 \tag{28}$$

where $Le=v/D_B$, is the Lewis number, $Nb=(\rho c)_p D_B\varphi_\infty/(\rho c)_f v$ denotes the Brownian motion parameter, $Nt=(\rho c)_p D_T(T_w-T_\infty)/(\rho c)_f vT_\infty$ represent the thermophoresis parameter.

## 3. Results and discussion

The set of nonlinear highly ordinary differential equations (9), (19), and (27) with the respective boundary conditions (10), (20), and (28) are solved numerically using Keller box method (Cebeci & Bradshaw, 2012), for the velocity, temperature and concentration fields. The computation is repeated until some convergence criterion is satisfied up to the desired accuracy of a $10^{-5}$ level. Comparison with the existing results published by Fang et al.

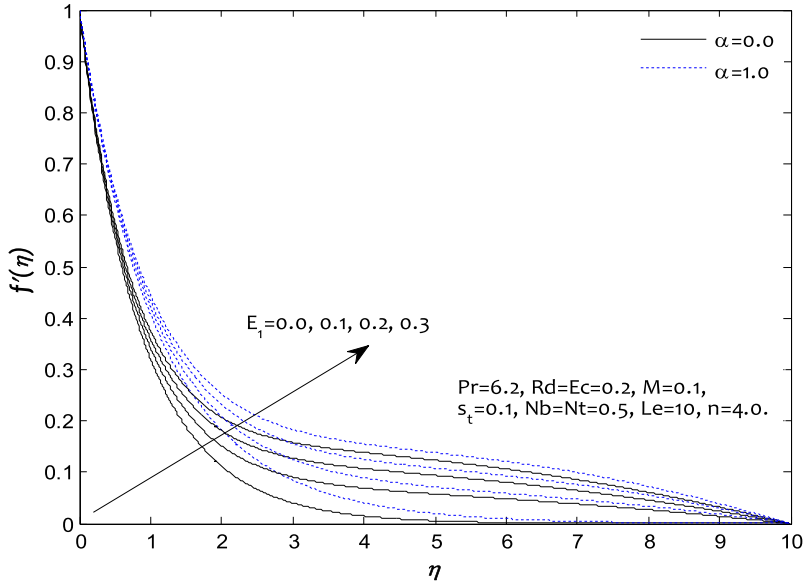


**Fig. 3.** Influence of $E_1$ on the velocity profile $f'(\eta)$.

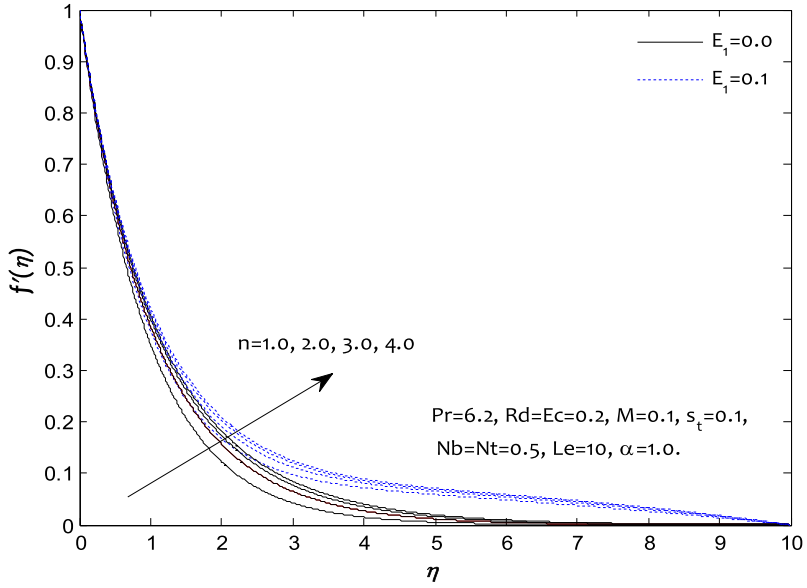


**Fig. 4.** Influence of $n$ on the velocity profile $f'(\eta)$.

(2012) shows a perfect agreement, as presented in Tables 1 and 2. Table 3 displayed the variation of the skin friction coefficient, and Table 4 displayed local Nusselt number in relation to magnetic field $M$, thermal radiation $Rd$, Eckert number $Ec$, Lewis number $Le$, Brownian motion $Nb$, thermophoresis $Nt$, Prandtl number $Pr$, power law index $n$, electric field $E_1$, and thermal stratification $s_t$ parameters. In Table 3, the skin friction coefficient increases by increasing $M, \& n$ while it decreases for higher values $E_1$ and $\alpha$. Generated numerical values of the local Nusselt number for different involving parameters are presented in Table 4. It is noted that the local Nusselt number decreases for higher values of $M, Rd, Ec, Le, Nt,$ and $s_t$, however it increases for higher values of $n, Pr,$ and $E_1$.

Figs. 2–4 displayed the dimensionless velocity fields for various values of magnetic field parameter $M$, electric field parameter $E_1$, and nonlinear stretching sheet parameter $n$. Variation in velocity with an increase in magnetic field parameter $M$ with effects of variable thickness can be seen from Fig. 2. It is noticed that an increase in $M$, the velocity profiles reduced close to the wall and suddenly increase near the stretching sheet surface as result of electrical force. The Lorentz force which acts as a retarding force tends to enhance the frictional resistance opposing the nanofluid movement in the hydrodynamic boundary layer thickness. In the case of presence of variable thickness, the velocity and momentum boundary layer is higher. The effects of electric field parameter $E_1$, on the velocity profiles, is presented in Fig. 3 with effects of variable thickness. Increasing in the values $E_1$ accelerate the nanofluid flow more significantly near the stretching sheet surface with thicker hydrodynamic boundary layer thickness. This is as result of Lorentz force that is arising due to an electrical force acting as accelerating force which tends to reduce the frictional resistance leading to shifting the stream away from the nonlinear stretching sheet. The velocity increase as the momentum boundary layer becomes thicker in the presence of variable thickness parameter

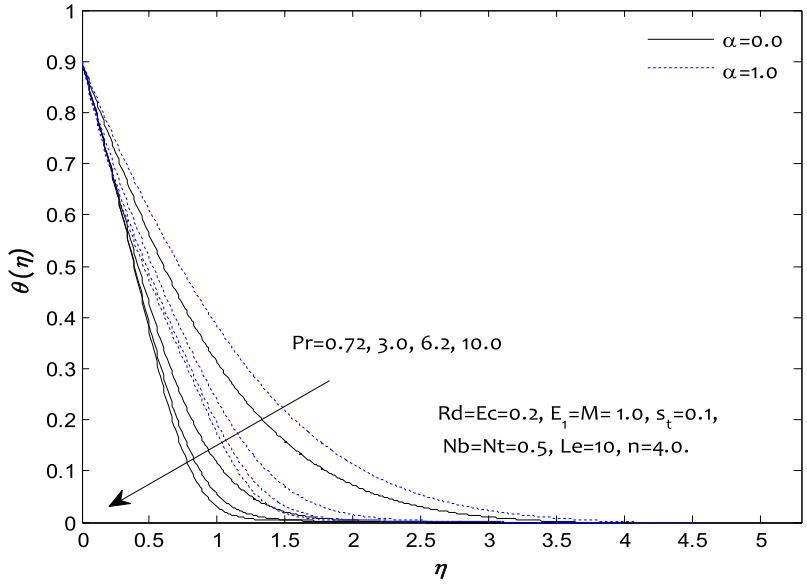


**Fig. 5.** Influence of $Pr$ on the temperature profile $\theta(\eta)$.

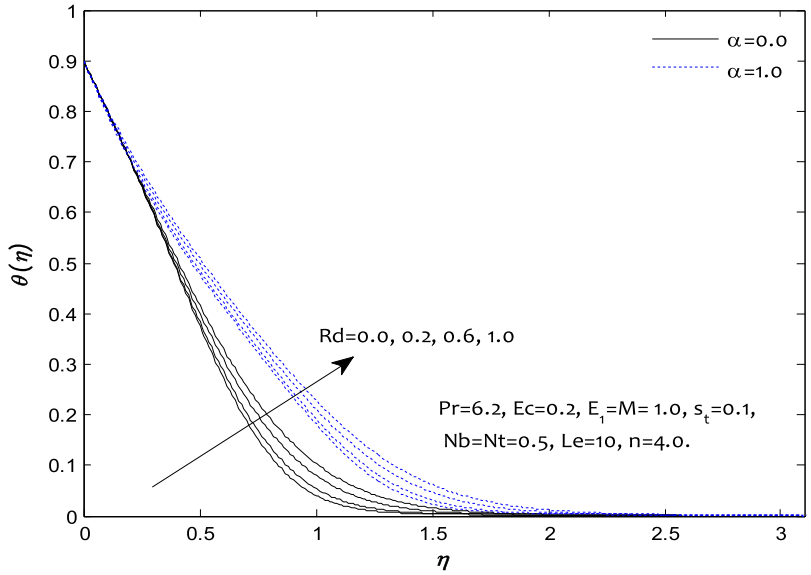


**Fig. 6.** Influence of $Rd$ on the temperature profile $\theta(\eta)$.

to that of absence. Fig. 4 portrays the influence of nonlinear stretching sheet parameter $n$ in the presence of electric field parameter ($E_1 = 0.1$) and absence ($E_1 = 0.0$). Higher values of $n$ resulted in an increase in the velocity profiles and thicker momentum boundary layer thickness. In the case of presence of electric field, the flow shifts away from the stretching surface at initial stage with an increase in the velocity field. The velocity gradient reduced as the nonlinear stretching sheet rises.

The variation of temperature field $\theta(\eta)$ for various values of Prandtl number *Pr*, thermal radiation parameter *Rd*, Eckert number *Ec*, and thermal stratification parameter $s_t$, is investigated in the Figs. 5–8. From Fig. 5, we examined for larger $Pr > 1$ momentum boundary layer thickness is greater than thermal boundary layer thickness with thicker thermal boundary layer thickness with a presence of variable thickness. Since Prandtl number is the momentum diffusivity to thermal diffusivity. The fluid temperature decreases close to the nonlinear stretching sheet surface significantly for an increase in the values of Prandtl number. The rate of heat transfer at the surface increase with increases in values of *Pr*. Radiation impacts on the temperature field is depicted in Fig. 6. An increase in values of *Rd* enhances the heat flux from the nonlinear stretching sheet which resulted in an increase in the fluid's temperature. Hence the temperature field and thermal boundary layer increase with an increase in *Rd*. In the absence of variable thickness, the thermal boundary layer thickness is lower compared to presence. The temperature gradient reduced for higher values of thermal radiation. Fig. 7 illustrate that temperature is an increasing function of the Eckert number *Ec*. The fluid temperature and thermal boundary layer thickness increase significantly in the presence of variable thickness. Eckert number is the ratio of kinetic energy to enthalpy. For higher values of *Ec*, kinetic energy rises with consequently enhances the nanofluid

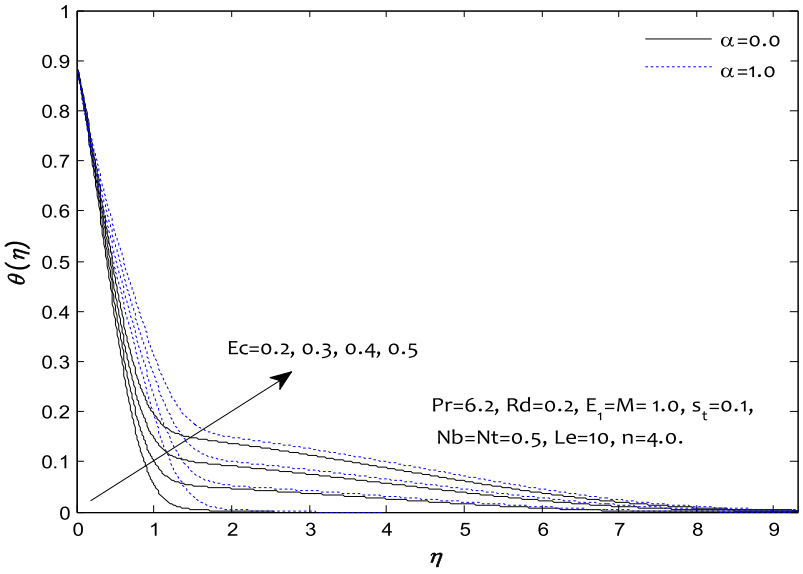


**Fig. 7.** Influence of *Ec* on the temperature profile $\theta(\eta)$.

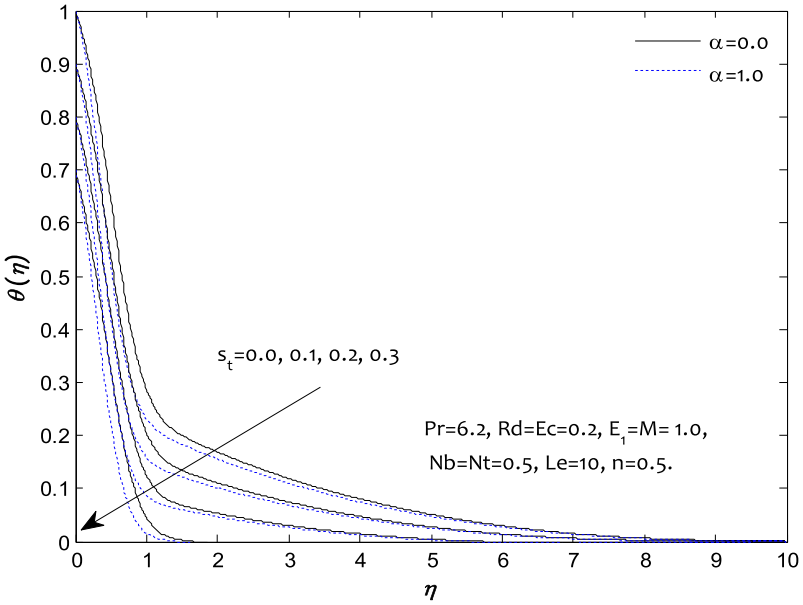


**Fig. 8.** Influence of $s_t$ on the temperature profile $\theta(\eta)$.

temperature. The rate of heat transfer at the surface reduced for much quantity of viscous dissipation. Fig. 8 is sketched to analyze the variation in temperature field for varying thermal stratification parameter $s_t$. It is worth notice that fluid temperature is a decreasing function of thermal stratification with a rise in variable thickness parameter. The effective convective potential that coexists between the nonlinear stretching sheet and the ambient nanofluid decreased with an increase in $s_t$. In view of this, the fluid temperature and thermal boundary layer thickness reduced for higher thermal stratification. The rate of heat transfer at the surface increases for an increase in the amount of thermal stratification.

Figs. 9–11 are plotted to examine the behavior of Brownian motion parameter *Nb*, thermophoresis parameter *Nt*, and Lewis number *Le* on the dimensionless nanoparticles concentration field $\phi(\eta)$. Fig. 9 it is obvious that the nanoparticle concentration and its solutal boundary layer thickness is smaller for larger Brownian motion parameter with thicker concentration boundary layer as resulted of variable thickness. The nanoparticle concentration gradient at the boundary wall is controlled passively at the surface by the expression of $(-Nt/Nb)$ and temperature gradient. The effects of thermophoresis parameter *Nt* on the concentration profile $\phi(\eta)$ is demonstrated in Fig. 10. It is noticed that the nanoparticle concentration increases with an increase in thermophoresis parameter and higher with variable thickness. This is as result of thermophoresis force developed by the rate of mass transfer at the surface creates a smooth flow far from the nonlinear stretching

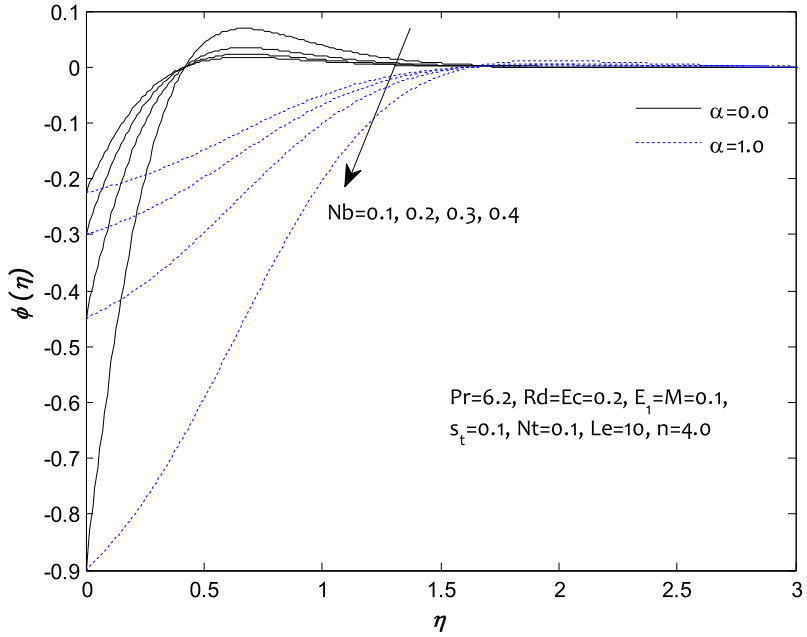


**Fig. 9.** Influence of *Nb* on the concentration profile $\phi(\eta)$.

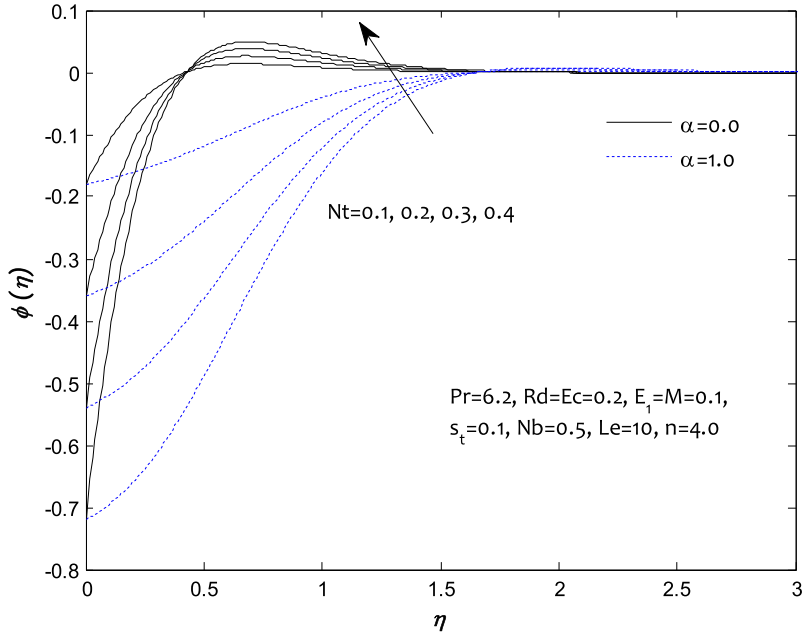


**Fig. 10.** Influence of *Nt* on the concentration profile $\phi(\eta)$.

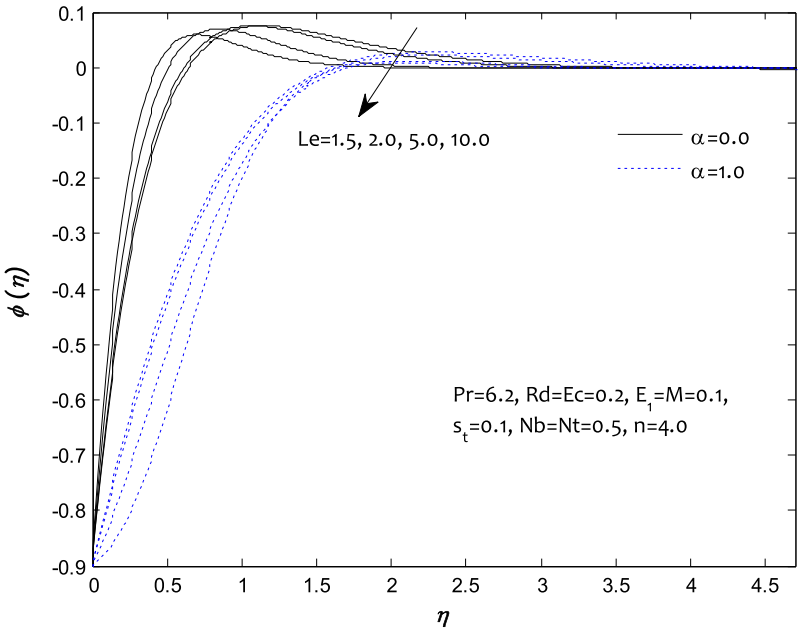


**Fig. 11.** Influence of *Le* on the concentration profile $\phi(\eta)$.

sheet surface. In view of this more heated fluid shift away from the surface and hence with much amount of thermophoresis, the fast flow from the nonlinear stretching sheet due to the presence of thermophoresis force resulting to enhancement in the nanoparticle concentration boundary layer thickness. The influence of Lewis number *Le* on nanoparticle concentration is revealed in Fig. 11. It is worth noticing that the nanoparticle concentration reduced significantly with higher values of Lewis number but thicker with variable thickness. This reduction in nanoparticle concentration and solutal boundary layer thickness is as results of the change in Brownian diffusion coefficient. It noted that higher values Lewis number associated to weaker Brownian diffusion coefficient. The concentration gradient increases with higher values of Lewis number.

## 4. Conclusion

The impact of thermal radiation and Joule heating due to the magnetohydrodynamic (MHD) flow of nanofluid against a nonlinearly stretching sheet with variable thickness are examined in the presence of thermal stratification. Thermal stratification and passively controlled nanoparticle concentration on the boundary condition in the presence of applied magnetic and electric fields makes this investigation novel one. The main conclusion of this study is stated as follows:

i High velocity is obtained for higher values of electric field and nonlinear stretching sheet.
ii The temperature reduces with increasing values of the thermal stratification parameter and Prandtl number.
iii Magnetic field effects on electrical conducting nanofluid suppressed the flow at the initial stage and after some distance enhances due to electrical force near the nonlinear stretching sheet surface which leads to enhancement of the skin friction coefficient.
iv The radiative heat transfer and viscous dissipation in the presence of variable thickness plays a dominant role in the temperature of the nanofluid.
v Lewis number and thermophoresis of nanoparticles reduces the nanoparticle concentration volume fraction for higher values but enhanced the mass transfer rate at the controlled surface.
vi Brownian movement and thermophoresis nanoparticle deposition in the presence of variable thickness and electric field reaches a significant role on the nanoparticle concentration volume fraction due to random movement of ultrafine nanoparticle suspended in the base fluid with passively controlled boundary at the wall.

## Acknowledgments

The authors would like to acknowledge Ministry of Higher Education and Research Management Centre, UTM for the financial support through GUP with vote number 11H90, Flagship grants with vote numbers 03G50 and 03G53 for this research.

## References

Alsaedi, A., Khan, M. I., Farooq, M., Gull, N., & Hayat, T. (2017). Magnetohydrodynamic (MHD) stratified bioconvective flow of nanofluid due to gyrotactic microorganisms. *Advanced Powder Technology, 28*(1), 288–298.
Besthapu, P., Haq, R. U., Bandari, S., & Al-Mdallal, Q. M. (2017). Mixed convection flow of thermally stratified MHD nanofluid over an exponentially stretching surface with viscous dissipation effect. *Journal of the Taiwan Institute of Chemical Engineers, 71*, 307–314.
Bhatti, M. M., Abbas, T., & Rashidi, M. M. (2017). Entropy generation as a practical tool of optimisation for non-Newtonian nanofluid flow through a permeable stretching surface using SLM. *Journal of Computational Design and Engineering, 4*(1), 21–28.
Cebeci, T., & Bradshaw, P. (2012). *Physical and computational aspects of convective heat transfer*. Springer Science & Business Media.
Choi, S. (1995). Enhancing conductivity of fluids with nanoparticles. *ASME Fluids Engineering Division, 231*, 99–105.
Daniel, Y. S. (2015a). Steady MHD laminar flows and heat transfer adjacent to porous stretching sheets using HAM. *American Journal of Heat and Mass Transfer, 2*(3), 146–159.
Daniel, Y. S. (2015b). Presence of heat generation/absorption on boundary layer slip flow of nanofluid over a porous stretching sheet. *American Journal of Heat and Mass Transfer, 2*(1), 15.
Daniel, Y. S. (2016a). Steady MHD boundary-layer slip flow and heat transfer of nanofluid over a convectively heated of a non-linear permeable sheet. *Journal of Advanced Mechanical Engineering, 3*(1), 1–14.
Daniel, Y. S. (2016b). Laminar convective boundary layer slip flow over a flat plate using homotopy analysis method. *Journal of the Institution of Engineers (India): Series E, 97*(2), 115–121.

Daniel, Y. S. (2017). MHD laminar flows and heat transfer adjacent to permeable stretching sheets with partial slip condition. *Journal of Advanced Mechanical Engineering, 4*(1), 1–15.
Daniel, Y. S., Aziz, Z. A., Ismail, Z., & Salah, F. (2017a). Effects of thermal radiation, viscous and Joule heating on electrical MHD nanofluid with double stratification. *Chinese Journal of Physics, 55*(3), 630–651.
Daniel, Y. S., Aziz, Z. A., Ismail, Z., & Salah, F. (2017b). Impact of thermal radiation on electrical MHD flow of nanofluid over nonlinear stretching sheet with variable thickness. *Alexandria Engineering Journal*.
Daniel, Y. S., Aziz, Z. A., Ismail, Z., & Salah, F. (2017c). Effects of slip and convective conditions on MHD flow of nanofluid over a porous nonlinear stretching/shrinking sheet. *Australian Journal of Mechanical Engineering*, 1–17.
Daniel, Y. S., Aziz, Z. A., Ismail, Z., & Salah, F. (2017d). Entropy analysis in electrical magnetohydrodynamic (MHD) flow of nanofluid with effects of thermal radiation, viscous dissipation, and Chemical reaction. *Theoretical and Applied Mechanics Letters*.
Daniel, Y. S., Aziz, Z. A., Ismail, Z., & Salah, F. (2017e). Numerical study of Entropy analysis for electrical unsteady natural magnetohydrodynamic flow of nanofluid and heat transfer. *Chinese Journal of Physics*.
Daniel, Y. S., & Daniel, S. K. (2015). Effects of buoyancy and thermal radiation on MHD flow over a stretching porous sheet using homotopy analysis method. *Alexandria Engineering Journal, 54*(3), 705–712.
Das, K., Sharma, R. P., & Sarkar, A. (2016). Heat and mass transfer of a second grade magnetohydrodynamic fluid over a convectively heated stretching sheet. *Journal of Computational Design and Engineering, 3*(4), 330–336.
Fang, T., Zhang, J., & Zhong, Y. (2012). Boundary layer flow over a stretching sheet with variable thickness. *Applied Mathematics and Computation, 218*(13), 7241–7252.
Farooq, M., Khan, M. I., Waqas, M., Hayat, T., Alsaedi, A., & Khan, M. I. (2016). MHD stagnation point flow of viscoelastic nanofluid with non-linear radiation effects. *Journal of Molecular Liquids, 221*, 1097–1103.
Hayat, T., Khan, M. I., Alsaedi, A., & Khan, M. I. (2016). Homogeneous-heterogeneous reactions and melting heat transfer effects in the MHD flow by a stretching surface with variable thickness. *Journal of Molecular Liquids, 223*, 960–968.
Hayat, T., Khan, M. W. A., Alsaedi, A., & Khan, M. I. (2017). Squeezing flow of second grade liquid subject to non-Fourier heat flux and heat generation/absorption. *Colloid and Polymer Science, 295*(6), 967–975.
Hayat, T., Khan, M. I., Farooq, M., Alsaedi, A., Waqas, M., & Yasmeen, T. (2016). Impact of Cattaneo-Christov heat flux model in flow of variable thermal conductivity fluid over a variable thicked surface. *International Journal of Heat and Mass Transfer, 99*, 702–710.
Hayat, T., Khan, M. I., Farooq, M., Alsaedi, A., & Yasmeen, T. (2017). Impact of Marangoni convection in the flow of carbon–water nanofluid with thermal radiation. *International Journal of Heat and Mass Transfer, 106*, 810–815.
Hayat, T., Khan, M. I., Farooq, M., Yasmeen, T., & Alsaedi, A. (2016). Stagnation point flow with Cattaneo-Christov heat flux and homogeneous-heterogeneous reactions. *Journal of Molecular Liquids, 220*, 49–55.
Hayat, T., Khan, M. I., Imtiaz, M., Alsaedi, A., & Waqas, M. (2016). Similarity transformation approach for ferromagnetic mixed convection flow in the presence of chemically reactive magnetic dipole. *Physics of Fluids, 28*(10), 102003.
Hayat, T., Khan, M. I., Waqas, M., & Alsaedi, A. (2017). Mathematical modeling of non-Newtonian fluid with chemical aspects: A new formulation and results by numerical technique. *Colloids and Surfaces A: Physicochemical and Engineering Aspects, 518*, 263–272.
Hayat, T., Khan, M. I., Waqas, M., Alsaedi, A., & Farooq, M. (2017). Numerical simulation for melting heat transfer and radiation effects in stagnation point flow of carbon–water nanofluid. *Computer Methods in Applied Mechanics and Engineering, 315*, 1011–1024.
Hayat, T., Khan, M. I., Waqas, M., Alsaedi, A., & Yasmeen, T. (2017). Diffusion of chemically reactive species in third grade fluid flow over an exponentially stretching sheet considering magnetic field effects. *Chinese Journal of Chemical Engineering, 25*(3), 257–263.
Hayat, T., Khan, M. I., Waqas, M., Yasmeen, T., & Alsaedi, A. (2016). Viscous dissipation effect in flow of magnetonanofluid with variable properties. *Journal of Molecular Liquids, 222*, 47–54.
Hayat, T., Nassem, A., Khan, M. I., Farooq, M., & Al-Saedi, A. (2017). Magnetohydrodynamic (MHD) flow of nanofluid with double stratification and slip conditions. *Physics and Chemistry of Liquids*, 1–20.
Hayat, T., Qayyum, S., Shehzad, S. A., & Alsaedi, A. (2017). Simultaneous effects of heat generation/absorption and thermal radiation in magnetohydrodynamics (MHD) flow of Maxwell nanofluid towards a stretched surface. *Results in Physics, 7*, 562–573.
Hayat, T., Rashid, M., Imtiaz, M., & Alsaedi, A. (2017). MHD effects on a thermo-solutal stratified nanofluid flow on an exponentially radiating stretching sheet. *Journal of Applied Mechanics and Technical Physics, 58*(2), 214–223.
Hayat, T., Shah, F., Alsaedi, A., & Khan, M. I. (2017). Development of homogeneous/heterogeneous reaction in flow based through non-Darcy Forchheimer medium. *Journal of Theoretical and Computational Chemistry*, 1750045.
Hayat, T., Waqas, M., Khan, M. I., & Alsaedi, A. (2016). Analysis of thixotropic nanomaterial in a doubly stratified medium considering magnetic field effects. *International Journal of Heat and Mass Transfer, 102*, 1123–1129.
Hayat, T., Waqas, M., Khan, M. I., & Alsaedi, A. (2017). Impacts of constructive and destructive chemical reactions in magnetohydrodynamic (MHD) flow of Jeffrey liquid due to nonlinear radially stretched surface. *Journal of Molecular Liquids, 225*, 302–310.
Hayat, T., Waqas, M., Shehzad, S., & Alsaedi, A. (2016). A model of solar radiation and Joule heating in magnetohydrodynamic (MHD) convective flow of thixotropic nanofluid. *Journal of Molecular Liquids, 215*, 704–710.
Hussain, T., Shehzad, S., Hayat, T., & Alsaedi, A. (2015). Hydromagnetic flow of third grade nanofluid with viscous dissipation and flux conditions. *AIP Advances, 5*(8), 087169.
Kandasamy, R., Mohammad, R., Zailani, N. A. B. M., & Jaafar, N. F. B. (2017). Nanoparticle shapes on squeezed MHD nanofluid flow over a porous sensor surface. *Journal of Molecular Liquids, 233*, 156–165.
Khan, M. I., Hayat, T., Khan, M. I., & Alsaedi, A. (2017). A modified homogeneous-heterogeneous reactions for MHD stagnation flow with viscous dissipation and Joule heating. *International Journal of Heat and Mass Transfer, 113*, 310–317.
Khan, M. I., Hayat, T., Waqas, M., & Alsaedi, A. (2017). Outcome for chemically reactive aspect in flow of tangent hyperbolic material. *Journal of Molecular Liquids, 230*, 143–151.
Khan, M. I., Hayat, T., Waqas, M., Khan, M. I., & Alsaedi, A. (2017). Impact of heat generation/absorption and homogeneous-heterogeneous reactions on flow of Maxwell fluid. *Journal of Molecular Liquids, 233*, 465–470.
Khan, M. I., Khan, M. I., Waqas, M., Hayat, T., & Alsaedi, A. (2017). Chemically reactive flow of Maxwell liquid due to variable thicked surface. *International Communications in Heat and Mass Transfer, 86*, 231–238.
Khan, M. I., Kiyani, M., Malik, M., Yasmeen, T., Khan, M. W. A., & Abbas, T. (2016). Numerical investigation of magnetohydrodynamic stagnation point flow with variable properties. *Alexandria Engineering Journal, 55*(3), 2367–2373.
Khan, M. I., Waqas, M., Hayat, T., & Alsaedi, A. (2017). A comparative study of Casson fluid with homogeneous-heterogeneous reactions. *Journal of Colloid and Interface Science, 498*, 85–90.
Khan, M. W. A., Waqas, M., Khan, M. I., Alsaedi, A., & Hayat, T. (2017). MHD stagnation point flow accounting variable thickness and slip conditions. *Colloid and Polymer Science*, 1–9.
Kumar, R., Sood, S., Sheikholeslami, M., & Shehzad, S. A. (2017). Nonlinear thermal radiation and cubic autocatalysis chemical reaction effects on the flow of stretched nanofluid under rotational oscillations. *Journal of Colloid and Interface Science*.
Kuznetsov, A., & Nield, D. (2013). The Cheng-Minkowycz problem for natural convective boundary layer flow in a porous medium saturated by a nanofluid: a revised model. *International Journal of Heat and Mass Transfer, 65*, 682–685.
Malik, M., Bilal, S., Bibi, M., & Ali, U. (2017). Logarithmic and parabolic curve fitting analysis of dual stratified stagnation point MHD mixed convection flow of Eyring-Powell fluid induced by an inclined cylindrical stretching surface. *Results in Physics, 7*, 544–552.
M'hamed, B., Sidik, N. A. C., Yazid, M. N. A. W. M., Mamat, R., Najafi, G., & Kefayati, G. (2016). A review on why researchers apply external magnetic field on nanofluids. *International Communications in Heat and Mass Transfer, 78*, 60–67.
Raju, R. S., Reddy, G. J., Rao, J. A., & Rashidi, M. (2016). Thermal diffusion and diffusion thermo effects on an unsteady heat and mass transfer magnetohydrodynamic natural convection Couette flow using FEM. *Journal of Computational Design and Engineering, 3*(4), 349–362.
Sheikholeslami, M., & Shehzad, S. (2017a). Magnetohydrodynamic nanofluid convection in a porous enclosure considering heat flux boundary condition. *International Journal of Heat and Mass Transfer, 106*, 1261–1269.
Sheikholeslami, M., & Shehzad, S. (2017b). CVFEM for influence of external magnetic source on Fe 3 O 4-H 2 O nanofluid behavior in a permeable cavity considering shape effect. *International Journal of Heat and Mass Transfer, 115*, 180–191.
Waqas, M., Farooq, M., Khan, M. I., Alsaedi, A., Hayat, T., & Yasmeen, T. (2016). Magnetohydrodynamic (MHD) mixed convection flow of micropolar liquid due to nonlinear stretched sheet with convective condition. *International Journal of Heat and Mass Transfer, 102*, 766–772.
Waqas, M., Khan, M. I., Hayat, T., Alsaedi, A., & Khan, M. I. (2017). Nonlinear thermal radiation in flow induced by a slendering surface accounting thermophoresis and Brownian diffusion. *The European Physical Journal Plus, 132*(6), 280.